ANGULAR RECONSTITUTION IN THREE-DIMENSIONAL ELECTRON MICROSCOPY: HISTORICAL AND THEORETICAL ASPECTS

M. van Heel[1,2,*], E.V. Orlova[1,2], G. Harauz[3], H. Stark[1,2], P. Dube[1,2], F. Zemlin[2] and M. Schatz[1,4]

[1]Department of Biochemistry, Imperial College of Science, Medicine and Technology, London, England
[2]Fritz-Haber-Institut der Max Planck Gesellschafft, Berlin, Germany
[3]Department of Molecular Biology, Genetics and Biophysics, University of Guelph, Guelph, Ontario, Canada
[4]Image Science Software GmbH, Berlin, Germany

Abstract

Angular reconstitution in combination with multivariate statistical techniques to classify and average the characteristic views of a molecule form a complete, self-contained methodology for the high-resolution three-dimensional (3D) structure analysis of uncrystallized macromolecules by electron microscopy. The angular reconstitution approach is based on the fact that two different two-dimensional (2D) projections of a 3D object always have a one-dimensional (1D) line projection in common. From the angles between such common-line projections, the relative Euler angle orientations of projections can be determined. Our single-particle electron microscopical approach has already yielded structures to resolution levels of ~10Å and no theoretical resolution limits are yet in sight.

The angular reconstitution approach was first presented ten years ago. A decade later, we can invoke hindsight to discuss the development of angular reconstitution in its historical context.

Key Words: Multivariate statistical analysis (MSA), automatic classification, hierarchical ascendant classification, three-dimensional (3D) reconstruction, angular reconstitution, macromolecular structure, Euler angles, sinograms, sinogram correlation functions.

*Address for correspondence:
Marin van Heel
Department of Biochemistry
Imperial College of Science, Medicine and Technology,
London SW7 2AY, England
                Telephone number: +44-171-594-5316
                        FAX number: +44-171-594-5317
                        E-mail: m.vanheel@ic.ac.uk

Introduction

Electron microscopy represents a very direct method for determining the structure of biological macromolecules, and complements the well-established technique of X-ray crystallography (cf. Blundell and Johnson, 1976). The micrographs record images of the object and not just their diffraction patterns and thus the classical "phase" problem of X-ray crystallography is non-existent in electron microscopy (EM). Modern electron microscopes routinely reach resolutions of ~2Å, which should be sufficient to elucidate the polypeptide backbone in proteins directly. Why then is it that X-ray crystallography still exists? The main problem in EM biological macromolecules is that of specimen preparation and of radiation damage. As information in the image "rains in" with the arriving electrons, the radiation damage exerted by those electrons onto the specimen gradually increases and by the time enough "light" has been shed on the object to produce a good signal-to-noise (SNR) image, the biological object has been reduced to ashes. Thus one is forced to collect a large number of copies of the molecule under study, each imaged under "low-dose" conditions, to subsequently average that large number of molecular images into noise-reduced averages.

In a set of many noisy images of an object, the noise at any position varies from image to image, but the desired feature information is the same. By averaging, the reproducible signal is enhanced with respect to the random background noise (cf. Misell, 1978; Frank, 1996). For such averaging procedures, regular aggregates of the molecules were obviously the first choice. In the late nineteen sixties and early nineteen seventies, image processing approaches for extracting two- and three-dimensional (averaged) information from regular aggregates were introduced mainly by the Cambridge group around Aaron Klug (DeRosier and Klug, 1968) with very impressive results. Three-dimensional reconstruction was applied first to helical fibers (DeRosier and Moore, 1970) which, by their mere nature, already correspond to a full tomographic tilt series of projections of the helix, and to icosahedral viruses (Crowther, 1971) whereby each viral image represents 60 different views of the object because of its high degree of symmetry.

The averaging procedure of a 2D crystal image

(Unwin and Henderson, 1975; Saxton and Baumeister, 1982; Henderson *et al.*, 1990) yields a two-dimensional (2D) projection image of the unit cell of the crystal often with a spectacularly improved signal-to-noise-ratio (SNR). The averaging of a 2D crystal of purple membrane embedded in glucose, where the sugar supports the protein by taking over the role of the bound water, for the first time offered a view of alpha helices traversing the membrane of a cell (Unwin and Henderson, 1975). Three-dimensional (3D) information may be obtained by combining many noise-free projection images of the unit cell and its environment seen from different directions obtained by tilting the specimen holder (Henderson and Unwin, 1975). One of the great landmarks in biological EM has been the elucidation of the atomic structure of bacteriorhodopsin by Henderson and co-workers (Henderson *et al.*, 1990). That success has inspired a renaissance of 2D crystallization of biological macromolecules (Jap *et al.*, 1992; Kühlbrandt and Downing, 1989; Kühlbrand *et al.*, 1994).

Crystallographic approaches based either on X-ray diffraction of 3D crystals or on electron microscopical images (our focus here) of 2D crystals have thus been used successfully in elucidating atomic resolution structures of biological macromolecules. The single major disadvantage of the crystallographic approaches is that they require crystals. Crystals may be difficult to obtain for a given macromolecule or, if they can be grown, may impose boundary conditions on the macromolecules which obscure the dynamic properties of the molecules. Single particle 3D methodologies for elucidating 3D structures thus inherently complement the crystallographic approaches which make them well worth pursuing even if the resolutions achievable are (or prove to be) lower than those obtained by the crystallographic approaches.

In analyzing electron micrographs of individual biological macromolecules we face a more complicated averaging problem than we face with 2D crystals. Single molecules are not held in a fixed relative orientation with respect to each other and thus have five degrees of freedom more than the molecules in the 2D crystal. Firstly, the molecules can lie anywhere in the plane of the object (**x,y**) in any possible in-plane rotational orientation (α). These three degrees of freedom apply to otherwise identical projection images. Moreover, the molecules have two degrees of freedom of out-of-the-plane rotations (β,γ) leading to fundamentally different projection images. Whereas, in principle, one may remove the in-plane degrees of freedom (**x,y,**α) by inter-image alignments (Frank *et al.*, 1978; Steinkilberg and Schramm, 1980; Frank *et al.*, 1981; Van Heel *et al.*, 1992a, Dube *et al.*, 1993), tackling the out-of-the-plane rotations (β,γ), requires the use of multivariate statistical classification. Such an automatic "multivariate statistical analysis (MSA)" classification consists of a data

compression phase (van Heel and Frank, 1980; 1981; Borland and van Heel, 1990), followed by a hierarchical ascendant classification procedure operating in the resulting compressed data space (van Heel, 1984a; 1989; Borland and van Heel, 1990; Frank, 1990; 1996). Averaging the images that are members of the same class finally yields high SNR class averages or "characteristic views" (van Heel and Stöffler-Meilicke, 1985). It is normally only after most of the noise has been removed from the electron microscopical projection images that one can actually start thinking about a 3D reconstruction.

The angular reconstitution technique (van Heel 1987; Goncharov and Gelfand, 1988; Farrow and Ottensmeyer, 1992; Radermacher, 1994) allows us to determine projection directions without making use of any instrumentally given projection directions. When one scans a patient's head in a computer tomograph, the X-ray source rotates around the patient and projection images through the patient's head are collected. For each projection image (or, typically, a projection line) one knows the instrumental projection direction or "tilt angle". Angular reconstitution, in contrast, uses the *data* in the projection images to find the relative spatial orientations of the projection images. The natural predecessor of the angular reconstitution technique is the common lines approach used routinely to reconstruct icosahedral viruses in three dimensions (Crowther, 1971). The more aggressively publicized comparison has, however, been that between the angular reconstitution approach and the Random Conical Tilt (RCT) technique (cf. Radermacher, 1988) as may be illustrated in the "Discussions with Reviewers" in (van Heel *et al.*, 1992b). In this paper we discuss the angular reconstitution approach, its historical development, and its relation to other techniques, whereas in the accompanying paper by (Schatz *et al.*, 1997), the focus is rather on practical aspects of the data processing.

An Optimally Aligned Data Set

Let us, purely for the sake of explaining the main angular reconstitution ideas, assume we already *know* the 3D structure we seek to reconstruct. From that 3D structure we can then calculate a large number of reprojections covering the "asymmetric triangle" of the corresponding pointgroup symmetry, as explained in the accompanying paper (Schatz *et al.*, 1997). Such "re-projections" are optimally translationally aligned with respect to the (common) 3D origin of the 3D structure and all have the best possible in-plane rotational orientation. When we use these reprojections as reference images for a Multi Reference Alignment (MRA: van Heel and Stöffler-Meilicke, 1985) of the full data set, we have an operation that results in an aligned data set in which the (**x,y,**α) variations are minimal:

an optimally aligned data set. From this aligned data set we can determine a set of "characteristic views" or class averages which will equally be optimally aligned. By starting our explanation with the end results of the analysis, we emphasize the iterative character of the overall angular reconstitution procedures (see below).

Moreover, extracting the characteristic views was already possible in 1985 (van Heel and Stöffler-Meilicke, 1985) and starting at this level of processing thus reflects the state of the art at that point in time. [Of course, since the reference images then did not result from a single 3D volume, the results of the MRA procedures were not optimally aligned in the sense that multiple origins (**x,y**) and multiple orientations (**α**) could coexist in the aligned data set (Schatz *et al.*, 1995).] The main problem that remained to be solved, at that time, was that of assigning Euler angles to the characteristic views such that the projection images could serve as input for the appropriate 3D reconstruction schemes (Harauz and van Heel, 1986b; Radermacher, 1988).

The Search for Angular Reconstitution

For as long as electron microscopists have been examining biological macromolecules, they have been trying to figure out the angles between microscopical projection images - often in visual and sometimes other ingenious ways - in order to interpret the results in three dimensions. Mechanical tilting of the specimen in the EM to inter-convert characteristic projection images was often applied successfully. The angular reconstitution problem can be rephrased as: given two or more projection images of the same 3D object, how can we find their relative projection directions if these are not known *a priori* from the experimental set-up?

When a person is presented with 2D projection images of a simple 3D object, there is a good chance that the person will recognize the underlying object (van Heel, 1987) and will readily "reconstruct" the object in his or her mind. Such an experience indicates that it should be possible to somehow relate the 2D projection data in terms of the 3D orientations in an analytical way. There indeed is such an analytical solution, which was found by two different groups independently (indicating that its time had come). As far as our group is concerned, it was one of those ideas that was associated with a clear starting point in time and place, as is described below.

One of the earliest papers we have found that formulates an analytical solution to finding the relative orientations of particles is that of Wrigley (1975), who suggested the use of particle outlines to determine relative orientations. Interestingly, Lake (1982) had a similar idea for using "commuting successive projections" for the 3D localization of antibody attachment sites on the surface of the *E. coli* ribosome. Kam (1980) formulated a full 3D reconstruction scheme based on intricate convulsions of angular harmonics, and applied it later to a virus structure (Kam and Gafni, 1985). Further schemes based on harmonic expansions were proposed (Vogel *et al.*, 1986; Provencher and Vogel, 1988; Vogel and Provencher 1988) but are not used in practice. Harauz and Ottensmeyer (1984a; 1984b) used model matching to orient individual nucleosomes for 3D reconstruction (see also Beniac and Harauz, 1995). Van Heel (1984b) and Harauz and van Heel (1986a) showed with model data that it was feasible to first assign Euler angles using a random number generator and then to iteratively refine the Euler angles assignments by correlation between the input projections and reprojections of the earlier 3D reconstruction(s). In spite of these various proposed approaches, something was still missing, and the air was still charged with a je-ne-sais-quoi. Something was waiting to happen...

And There It Is!

After spending several days in mid-September 1985 at an X-ray crystallography meeting in Bischenberg, Elsaß, a stressed MvH traveled to Konstanz to a joint meeting of the German, Austrian and Swiss Electron Microscopical Societies. He spent the greater part of the night thinking about how to reconstruct the *Lumbricus terrestris* hemoglobin from its characteristic views; and the idea dawned at the actual dawn. After MvH's presentation the next day, Andreas Engel posed a question concerning the Euler angle determination and MvH, in his answer, referred to his sleepless night which may have brought the solution. That night was historical also for another author of this paper (FZ). In his room in the same hotel at the same conference site, he had no problems with his sleep and so did not notice the burglar who quietly entered his room to relieve him of his watch. MvH returned to Berlin full of excitement and got right to work. His post-doctoral associate at the time, GH, recalls MvH throwing himself into programming, asking our gifted instrument maker Peter Tesky to build a contraption consisting of three metal angles to demonstrate common-tilt-axes in real space, sticking pins into styrofoam spheres to pinpoint, literally, Euler angle direction vectors, and perusing mathematical tomes for obscure spherical trigonometric formulae. The algorithmic framework gradually became implemented over the fall of 1985, and throughout the following winter and spring.

The angular reconstitution idea was first presented publicly at the 44th Annual Meeting of the Electron Microscopical Society of America (EMSA) in Albuquerque in August of 1986. No abstract was submitted for this conference but a full paper was submitted a few weeks later (van Heel, 1987). The next presentation was at the 6th

Pfefferkorn Conference (April 1987) on "Image and Signal Analysis in Electron Microscopy" in Niagara Falls, Canada (van Heel and Harauz, 1988). After his 1987 paper was in print, MvH learned in a letter from Prof. Vainshtein, that he and his coworker had presented virtually the same idea in a Russian publication (Vainshtein and Goncharov, 1986a). Their idea was presented at the XIth International Congress on Electron Microscopy in Kyoto in September 1986 (Vainshtein and Goncharov, 1986b), and later published as a full paper in English (Goncharov and Gelfand, 1988).

The Angular Reconstitution

Problem *per se*

A whole generation of electron microscopists had been deriving 3D models of macromolecules by simply looking at the different views obtained from a macromolecule in an EM sample, for example, of the *E. coli* ribosome (cf. Lake, 1982). Such intuitively derived models gave rise to vivid controversies since objective criteria by which to judge the quality of the models were largely lacking. Nevertheless, the intuitive idea that two or more different projections of the same 3D volume contain partially the same information and that it is possible to *a posteriori* find their relative orientations is correct, and angular reconstitution provides methodological basis for that search. The theoretical abstraction one can derive from the half intuitive interpretations is the "common-tilt-axis" or "common-line-projection theorem" (van Heel, 1987). As will be discussed below, this theorem is the real-space equivalent of a similar theorem in Fourier space, the "common-central-line theorem" (Crowther, 1971).

The common-line-projection theorem states that two different 2D projections of a 3D object always have a one-dimensional (1D) line-projection in common. As we can project a 3D object onto a plane to produce a 2D projection image (the electron microscope does this very effectively for us), so we can project a 2D image onto a 1D line in any direction within the plane of the 2D image. As an example, the 3D model object shown in Figure 1a is first projected onto 2D planes (Fig. 1b) along the viewing direction used in Figure 1a. For each of these 2D projection images one can subsequently calculate all possible 1D projection images and mount them over each other in a 2D image (Fig. 2, second row) called a "sinogram" (cf. van Heel, 1987).
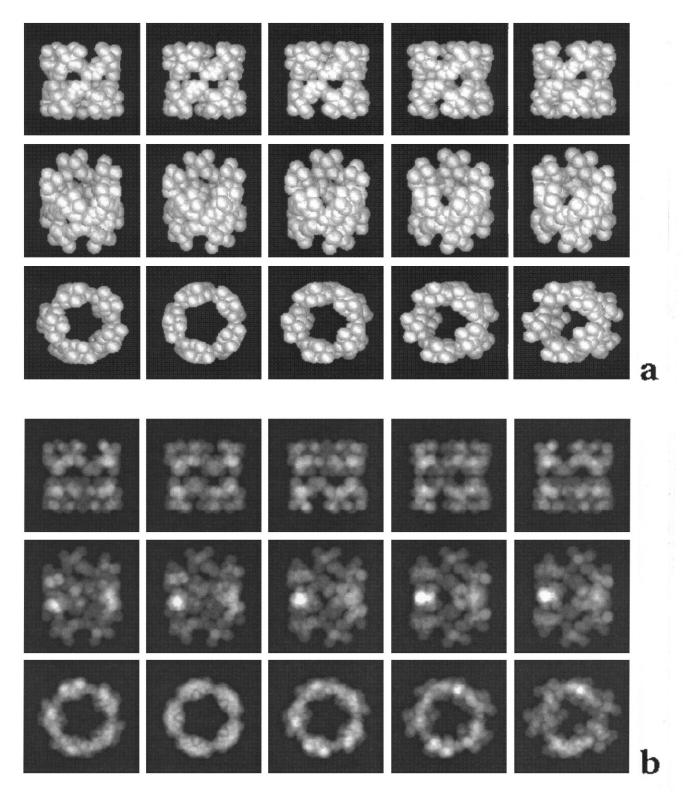
The common-line-projection theorem thus states that two sinograms (derived from two 2D projections) must have at least one line in common (horizontal lines in Figure 2, second row). Thus, we can search for that common-line projection by comparing ("correlating") each line in sinogram #1 with each line in sinogram #2 in a "sinogram correlation function", of which two are depicted in Figure 3. Since the sinograms in Figure 2 and 3 are calculated over a

Figure 1 (*on facing page*). (**a**) Stereo views of the D5 pointgroup symmetry 3D model used to explain the basic principles of "angular reconstitution". Using the IMAGIC (van Heel *et al.* 1996) command THREED-MODEL a three dimensional volume was generated which contains a number of spherical shapes defined by a set of X-Y-Z co-ordinates. A D5 pointgroup symmetry structure has a 5-fold axis (third row, second frame), typically placed along the Z-direction, and five 2-fold axis, perpendicular to the 5-fold axis, and separated by 72° intervals (first row, second frame). The images are shown as continuous stereo sequences implying that each horizontally neighbouring pair of images forms a stereo pair. (**b**) Projection images of the D5 pointgroup symmetry 3D model shown in Figure 1a. The projection directions are the same as the viewing direction in Figure 1a. In projection the symmetry axes of the D5 pointgroup symmetry structure can also be seen directly. The 5-fold axis is evident from the figure in the third row, second frame, and the 2-fold axis of the structure is visible in the figure in the first row, second frame.

360° range, a 2-fold redundancy in the data occurs and the sinogram correlation function will have *two* identical peaks for each pair of matching lines in the sinograms. (The sinogram line at angle φ is the mirror version of the line at angle φ ± 180° of the same sinogram).
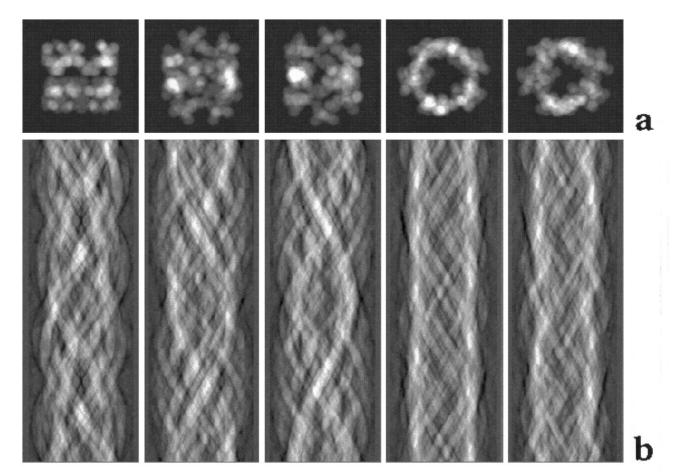
The relative *in-plane* orientations between the projections can be determined from the angles between these common-line-projections. Finding the correct in-plane orientation between the two 2D projections leads to a strong reduction in the number of open choices for the Euler angles (α, β, γ) that can be assigned to each of the projection images. For asymmetrical objects, a minimum of three projections is required (not related by tilting around a single axis) to entirely determine the relative orientations of the projections. For a highly symmetrical object, like the D5 model structure shown in Figure 1a, a single projection image (Figure 1b) already fully fixes its orientation since a single projection of a D5 symmetric object already corresponds to 10 *different* projections of the same object and that system is thus over-determined from the beginning. Because of the D5 symmetry of the model structure, the 2-fold redundancy of the sinogram correlation function translates to a total of $2 \times 10 = 20$ maxima in the correlation function (indicated by black dots in Figure 3).

We first embarked on solving the Euler angle problem using an algorithm that followed the analytical formulas to solve, essentially, the mathematics of classical spherical triangulation (cf. van Heel, 1987). This approach turned out to be quite error prone and the error message that drove GH/MvH in the years 1986-1988 was: "Schwarz's inequality

violated!" Schwarz's inequality rule is violated when the sum of two sides of a triangle is shorter than the third one. We first sought to solve what seemed to be the simplest problem, that of the asymmetric molecule requiring the smallest programming effort. However, the simplest cases turned out to be rather those of highly symmetric molecules like the D6 symmetric hemoglobin of *Lumbricus terrestris* (Orlova and van Heel, 1994; Schatz *et al.*, 1995), or viruses

Figure 2: Some 2D projection images of Figure 1b converted to "sinograms". The 2D projection images shown in the first row are here projected down further onto single lines ("line-projections"). The collection of all possible line-projections of a 2D image over an angular range for 0-360° forms a "sinogram" (lower row).

with icosahedral symmetry in which the redundancy in the data makes the programs converge rapidly.

It was only after we implemented "brute force" algorithms that search over all possible orientations of symmetric or asymmetric particles (van Heel *et al.*, 1992b) that the algorithmic approaches stabilized. Moreover, in the early phases, we believed we were limited by preferred orientations of the molecules with respect to the support film (cf. van Heel, 1987) and even in 1992 we still envisaged the use of small tilts of the specimen holder in order to further randomize the orientation of the molecules in the specimen (van Heel *et al.*, 1992b). Once the programs, and especially the iterative procedures listed below, reached maturity (Serysheva *et al.* 1995) preferred orientations turned out hardly to represent a problem at all (see Discussion). With highly symmetric structures, the redundancy in the data not only makes the programs converge rapidly but also the quality criteria, then measured over a large number of symmetry-related peaks, become

very sensitive against departure from an ideal behavior. Thus, poor class averages may be identified promptly and excluded from further processing more easily than with asymmetric structures. Historically, it was only *after* the programs had been used extensively for studying symmetric structures — we used the *Lumbricus terrestris* hemoglobin structure (Schatz *et al.*, 1995) for years for methodology development — that we successfully revisited the case of the asymmetric molecule, the 70S ribosome of *E. coli* (Stark *et al.*, 1995, 1997).

Iterative Refinements

In our deliberations we have reached the point where we have good SNR class averages with Euler angles assigned to them, and we therefore calculate a (new) 3D reconstruction. This new 3D reconstruction is then used directly to generate a *small* set of projection images (10-30), with which "reprojections" the Euler angle assignments of
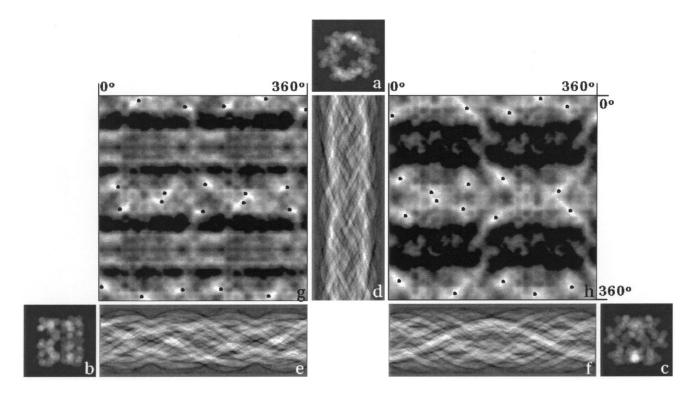
Figure 3: Sinogram correlation functions. Two sinograms calculated from two 2D projections of the same 3D structure have - at least - one line in common. To search for the line projections that two sinograms have in common, the two sinograms are compared line by line in so-called sinogram correlation functions (van Heel, 1987). In this illustration, we start with three different projection images (**a**, **b**, **c**). For these three projection images the corresponding sinograms have been calculated (**d**, **e**, **f**). The sinogram correlation functions, finally, are calculated by a line by line correlation of the corresponding sinograms, i.e., sinogram correlation function **g** is calculated by correlating sinograms **d** and **e**, whereas sinogram correlation function **h** is calculated by correlating sinograms **d** and **f**. The black dots in the sinogram correlation functions are markers to indicate the global maximum found for the Euler angle assignment for this set of three projections within the constraints imposed by the D5 pointgroup symmetry. The global maximum is found by searching for all symmetry related peaks in all relevant sinogram correlation functions simultaneously. Note that this illustration can also be used for explaining the concept of an anchor-set Euler angle assignment (see: Iterative refinements). Suppose projection image **a** is a somewhat noisy class average (rather than the model projection it actually is), and suppose we already had a preliminary 3D model of the molecule we are interested in. We can then assign Euler angles to the class average (**a**) by finding the global maximum in all its cross sinogram correlation functions (**g**, **h**) with respect to projections (**b**, **c**) of the earlier 3D model. In a real situation, we would not use just two (re)projections of the preliminary 3D model as an anchor set but typically 10-30 reprojections.

---

the class averages are refined. This small set of reprojections is called an "anchor set" (Orlova and van Heel, 1994; Schatz *et al.*, 1995, 1997). An anchor set of projection images is internally fully consistent since it is derived from the same 3D volume, and it thus represents a better frame of reference for assigning Euler angles than do the original set of class averages themselves. Thus, the class averages are assigned refined Euler angles by calculating the "cross" sinogram correlation functions with respect to the anchor set exclusively and a new 3D is calculated based on the same class averages.

Once we have the latter refined 3D structure available, we are back at the starting point of our deliberations: we have a 3D structure from which we generated a *large* number of reprojections (100-500, uniformly covering the asymmetric triangle) to be used as reference images for realigning the entire data set using a renewed MRA procedure. This procedure leads to an improved overall ("optimal") alignment of the full data set of raw molecular images. Using MSA data compression and automatic classification we can now produce better class averages in the sense that the improved classes contain fewer

misaligned images and contain (projection) images representing a narrower range of Euler angles (**β,γ**). Typically, one will, in the course of the procedures, use an increasing number of classes to reduce the range of Euler angles covered per class. Averaging too many molecular images into a class implies averaging over a relatively large range of Euler angle directions and that will obviously lead to a smearing out of the high-frequency information and to a loss in resolution in the resulting 3D reconstruction.

For historical reasons, we now go back to an earlier iterative procedure proposed by some of us, either as a complete Euler angle assignment procedure (van Heel, 1984b; Harauz and van Heel, 1986a) or as a refinement approach for Euler angles assigned by other techniques ("model matching": Harauz and Ottensmeyer, 1984a; 1984b). These procedures were based on the correlation between original images and a large number of reprojections of a preliminary 3D reconstruction, very much like the many reprojections we now use as references for our current MRA refinement. The Euler angles of the input projection images were, in these earlier procedures, assigned to the Euler angles of the reprojection which correlated best with that input image. Variants of this Euler angles assignment scheme have become quite popular recently (see Discussion).

We have now (cf. Orlova and van Heel, 1994) subdivided this earlier procedure into some six or seven separate procedures: (**a**) a full MRA of the data set with respect to a large set of reference images which are reprojections from a preliminary 3D reconstruction; (**b**) the MSA classification of the re-aligned full data set; (**c**) Euler angle assignment to the new *class-averages*, rather than to the raw noisy input images (usually), with respect to an anchor set derived from the previous 3D reconstruction; (**d**) 3D reconstruction using the new class-averages; (**e**) generation of a new anchor set from the new 3D; (**f**) reassignment of Euler angles to the new class-averages using the new anchor set; and, finally, (**g**) calculation of a new 3D reconstruction. The new approach is clearly more elaborate than our earlier one, but, at the same time, produces superior results.

Note that we chose an optimally aligned electron microscopical data set as our starting point. By doing so, we avoided discussing the centering of the data set in terms of the in-plane translations (**x,y**) and rotation (**α**). We originally expected the 3D centering of the data set to be an important problem and we designed an approach which used Self Correlation Functions (SCFs), which are, per definition centered in (**x,y**) (van Heel *et al.*, 1992b), to solve that problem. Although we do apply centering procedures to our data (see: Schatz *et al.*, 1997), the centering problem is *de facto* a subordinate problem that is automatically dealt with in the course of the iterative MRA refinements. The reprojections used to realign the full data set are, per defini-

tion, centered and thus all good classes resulting from the subsequent MSA classification are equally well aligned.

Electron Microscopy and Specimen Preparation

It may seem strange to discuss the electron microscopical aspects of the angular reconstitution technique towards the end of this paper. Specimen preparation is one of the most important aspects of our procedures, certainly now that the computation techniques are in place and stable. Single molecules were traditionally imaged contrasted with a thin layer of negative stain, which process typically forms a meniscus of small crystals around the molecules on a carbon-film support film (cf. Fernández-Moran *et al.*, 1966). These techniques were the first techniques that allowed systematic studies of large macromolecular structures, but the techniques had a number of inherent limitations: strong flattening artifacts can occur at the carbon foil interface (cf. Cejka *et al.*, 1991; 1992), preferential attachment often dictates that one sees just a low number of specific views, and, moreover, drying and/or radiation damage artifacts that distort the 3D information in unpredictable ways. The real problem, however, was not that the techniques as such were bad, but rather that the computational techniques to objectively *evaluate* the results were still largely lacking. The consensus rule of thumb that negative stain limits the attainable resolution to ~25Å is a perceived limitation that lacks hard supporting evidence.

With the advent of low-dose (Unwin and Henderson, 1975) and cryo-electron microscopy (Adrian *et al.*, 1984; Dubochet *et al.*, 1988) in connection with specimen embedding in glucose and in vitreous water, respectively, new light was shed on electron microscopy of biological macromolecules. With these novel techniques now well established, we must now revisit the earlier "negative stain" specimen preparation techniques. Indeed, by using combinations of glucose, negative stain and vitreous ice, we have recently been able to achieve a better than 15Å resolution on the Keyhole Limpet Hemocyanin type 1 (KLH1) (Orlova *et al.*, 1997) and even ~10Å on another sample (manuscript in preparation).

Comparison with Other Techniques

While discussing the angular reconstitution approach we have mentioned other techniques for studying 3D structures of single particles. Some recent publications must still be mentioned here (van Dyck, 1989; Salzman, 1990). A further noteworthy development was the application of quaternionic mathematics to calculation of rotation matrices (Farrow and Ottensmeyer, 1992; 1993; Harauz, 1990). We now want to focus on the other main EM techniques for determining the 3D structure of single particles.

Single particle tilt series

The first efforts to render the analysis of single particles more objective stemmed from the group of the late Walther Hoppe in Martinsried, Germany. The Martinsried group produced 3D reconstructions of fatty acid synthetase (Hoppe *et al.*, 1974) and of the *E. coli* ribosomal subunits (Oettl *et al.*, 1983) by tilting the grid in the electron microscope. The very first 3D reconstruction of a ribosome based on a tilt-series reconstruction that we are aware of was one by Gordon and coworkers (Bender *et al.*, 1970). The resolution in the 50S reconstruction of the Martinsried group (Oettl *et al.*, 1983) of around ~20Å was noteworthy and the "network of channels" found in that work does not disagree with more recent results (Yonath and Berkovitch-Yellin, 1993; Stark *et al.*, 1995); a lower threshold will, however, make the channels disappear (Frank *et al.*, 1995). However, the exposure level needed to collect the tilt series of individual macromolecules was considerable and the conventional microscopical techniques applied (i.e., air-dried uranyl acetate, room temperature EM) made it difficult to interpret the results in terms of the underlying biological structure.

Three-dimensional structures of single particles calculated by this technique, such as the 70S *E. coli* ribosome, continue to appear (Öfverstedt *et al.*, 1994); however, the interpretable resolution is often disappointing and, although the resolution claimed in this example is ~60Å, it is hardly possible to distinguish between the small and the large ribosomal subunits. Tilt series experiments are the technique of choice when reconstructing a unique structure such as the human chromosome (Harauz *et al.*, 1987). The most advanced and promising approach in tilt-series tomography is the computer-controlled cryo-tomography approach from the group around Wolfgang Baumeister in Martinsried (cf. Dierksen *et al.*, 1992).

Single particle 3D reconstructions by tilt-series tomography has some inherent disadvantages in comparison with the zero-tilt angular reconstitution technique. Tilting the specimen holder is a macroscopic operation which may cause changes in the specimen, causes defocus gradients within the image, and often is associated with significant defocus changes *between* the images of the series. As a consequence, the effective resolution in the resulting 3D reconstructions will normally be significantly lower than the achieved resolution with the same experimental effort with the angular reconstitution approach. Apart from possibly the newly refined approach from Martinsried, tilt series tomography with multiple exposures of the same specimen area require a much higher total electron exposure on each individual molecule, leading to a deterioration of the fine details in the biological macromolecules.

Random Conical Tilt (RCT)

The random conical tilt (RCT) approach was also born in the mid-eighties (Radermacher *et al.*, 1987a; 1987b; Radermacher, 1988). The RCT is a tilt-series approach, but here one avoids reconstructing each particle individually from an extended multi-exposure tilt series. One tilted as well as one untilted image of each specimen area is collected, of molecules that exert a preferred orientation on the support film. Thus, one creates a data set where the first Euler angle is simply the planar rotation angle of the molecule in the untilted image, and the second Euler angle is the specimen-holder tilt angle (the third Euler angle is zero). Thus, one single 3D reconstruction is performed integrating the information from many (~500) molecular images, whereby each image is exposed to the radiation only twice. Because of the largely reduced level of exposure, this technique is normally much better than the full tilt-series reconstructions discussed above.

It is often argued that the RCT is a *single* exposure technique, since only the first, less damaged image is used for the 3D reconstructions, whereas the alignment parameters are taken from the second, untilted image. However, this argument in only true to a limited extent: since the molecules in second micrograph have suffered more radiation damage, the alignment parameters derived from that image cannot be as good as those taken from a first exposure. Moreover, the argument discussed above in the context of single particle tilt-series reconstructions that the object as a whole may have changed due to the macroscopic tilt applied to the grid also applies to RCT reconstructions (independent from the hitherto unsolved problems of the defocus differences between the tilt pair members). The RCT technique was proposed more or less simultaneously with the angular reconstitution technique, but the RCT technique was simpler to implement and a substantial number of structures at the 30-50Å resolution level were elucidated before the angular reconstitution technique became fully operational. The latter zero-tilt reconstruction technique has significant advantages over the RCT technique in terms of both ease of operation and attainable resolution (van Heel *et al.*, 1992b, Schatz *et al.*, 1995).

Albany Zero Tilt (AZT) approaches

Interestingly, the Albany group around Joachim Frank has recently moved away from tilt series reconstructions by extending the RCT technique with post processors which use zero-tilt images *not* necessarily stemming from the original double exposure RCT data set. Two types of post-processors were proposed by this group: (1) correlations of original microscopical images with reprojections covering the unit sphere (Penczek *et al.*, 1994); and (2) correlations of original microscopical images through their "Radon transforms", with the Radon transforms of (a

small number of) reprojections of a preliminary 3D reconstruction (Radermacher, 1994).

The refinement technique proposed by Penczek *et al.* (1994) is, apart from the details of how the input images are correlated to the reprojections of the preliminary 3D volume, identical to the earlier techniques proposed by some of us (Harauz and Ottensmeyer, 1984a,b; van Heel, 1984b). The second refinement technique (Radermacher, 1994) uses correlations between "Radon transforms" rather than the "sinograms" used by us (van Heel, 1987). This alternative nomenclature is used to indicate exactly the same concept. Moreover, their alternative nomenclature is confusing because the sinogram is the *discrete* form of the Radon transform. The sinogram nomenclature has been in use since the beginning of conventional computerized tomography. In the context of Euler angle assignments to random oriented particles the sinogram nomenclature was used from the beginning (van Heel, 1987). Because of the alternative nomenclature used in the Radermacher (1994) paper, the reader may not notice that the technique is *de facto* merely a variant of the angular reconstitution method. The "3D Radon transform" in Radermacher (1994) is, in our nomenclature, a collection of sinograms derived from a (small) set of reprojections from a preliminary 3D reconstruction, in other words sinograms derived from an anchor set.

Both RCT extensions proposed by the Albany group have been used as "stand-alone" solutions by us. Although their new techniques are clearly converging toward our approaches, some differences still remain. One difference is that the Albany group assigns Euler angles to the raw images but we normally use class averages (MSA classifications) [in their latest publication the group now also resort to the use of class averages (Penczek *et al.*, 1996)]. Another difference is our extensive use of multi reference alignments (MRA) explained above and in the companion paper (Schatz *et al.*, 1997). The differences between the angular reconstitution approach and the RCT approach have been discussed loudly (see also the discussions appended to: van Heel *et al.*, 1992b). The predecessor of our technique, however, is not so much the RCT technique as the common-central-lines approach by Crowther (1971).

Common lines and icosahedral viruses

The 3D analysis of icosahedral viruses (Crowther *et al.*, 1970; Crowther, 1971) was certainly one of the first successful single particle analysis techniques. The central-section theorem (DeRosier and Klug, 1968) states that the 2D Fourier transform (FT) of a 2D projection through a 3D density corresponds to a 2D "central section" through the 3D Fourier transform of the 3D density. From this it follows that the 2D FTs of two different 2D projections of the same 3D volume share at least one central line, the common-central-line (short: "common line"). When an object has

icosahedral symmetry, each general projection image corresponds to 60 different projection images of the 3D volume! Thus, the FT of each projection image of an icosahedral virus will cross itself 59 times in Fourier space and each projection image thus has 59 central lines in common with itself.

As was pointed out extensively in the first angular reconstitution paper (van Heel, 1987), there is a complete equivalence between the *Fourier space* common- central-lines ideas and the *real space* common line projection ideas. Both ideas start with the real-space 2D projection of a real-space 3D object. With the angular reconstitution technique one then stays in real space, and calculates 1D projections from the 2D projection images (the collection of all possible 1D projections of a 2D image form "sinograms"). The 1D projections are real functions and are calculated in real space. With Crowther's (1971) approach one first moves to Fourier space by calculating the 2D FT of the 2D projection image. In the 2D FT, one then searches for central lines crossing the origin in order to "common-central-lines". The central lines in the 2D FT are simply the 1D FTs of the real space line projections. There are some practical advantages in dealing with the information in its *real* form rather than in its *complex* Fourier transformed form, but both forms are, theoretically speaking, identical. For example, the sinograms can directly be displayed as a density (van Heel, 1987; Serysheva *et al.*, 1995) whereas the Fourier space central lines are complex, i.e., characterized by both a phase and an amplitude, and thus need two curves to be displayed.

As mentioned earlier, we normally work with class averages rather than directly with the microscopical data because of SNR considerations. The only exception to that rule has hitherto been the analysis of structures with icosahedral symmetry (manuscript in preparation) whereby each single projection image already exerts a 60-fold redundancy which helps the procedures to converge promptly. In retrospect, it is understandable why the classical "common lines" approach was so successful in analyzing icosahedral viruses, but was never seriously applied to macromolecules with general pointgroup symmetries. Structures with much lower symmetry levels, such as the Ca^{2+}-release channel with C4 pointgroup symmetry (Serysheva *et al.*, 1995; Orlova *et al.*, 1996), would have been virtually impossible to analyze without the SNR improvements obtained in the class averages.

Refinement techniques have also been introduced for studying icosahedral viruses. Correlation between input viral images and a large number of reprojections of a preliminary 3D reconstruction have been used to refine Euler angles assignments of the input images (Cheng *et al.*, 1994). To save computing time these authors convert the input images and the reprojections to a rotationally invariant form (cf. Schatz and van Heel, 1992) and thus do not perform the

full correlation (Harauz and Ottensmeyer, 1984a; 1984b; Van Heel, 1984b), an approach which works well with roughly spherical viruses. Crowther *et al.* (1994) have also introduced the use of a small number of reprojections from a preliminary 3D reconstruction (only 3 were used in this publication) to then assign Euler angles to an input image by studying the "cross-common-lines" of that image to these reprojections, an approach which is identical to our anchor set approach discussed above.

Conclusions and Perspectives

A sweep through one of our dusty bookshelves revealed a paper-bound, home-printed Proceedings of a 1975 International Seminar on Biomolecular Electron Microscopy (Kleinschmidt, 1975). One of the papers in this volume was by Peter Ottensmeyer and was entitled "Structure determination of unstained macromolecules below 10Å today, in three dimensions tomorrow - a practical exposition of dark field electron microscopy". "Tomorrow" has taken some time to come! It has required an improvement in specimen preparation technique, in low-dose electron microscopy, and, above all, in 3D image processing techniques, the subject of this paper.

The angular reconstruction approach is currently one of the most successful approaches; it was already used to solve numerous structures at the 10-30Å resolution level since it became fully operational in 1993-1994 (Serysheva *et al.*, 1995; Dube *et al.*, 1995; Orlova and van Heel, 1994; Orlova *et al.*, 1996, 1997, Schatz *et al.*, 1995; Stark *et al.*, 1995, 1997). A direct descendant angular reconstruction approach, the IQAD (iterative quaternionic algorithmic determination), has also been used to elucidate a number of structures in low-dose, low-temperature (Czarnota *et al.*, 1994), and in the high-dose, room-temperature realm (Bazett-Jones *et al.*, 1996; Czarnota and Ottensmeyer, 1996).

Because of its experimental simplicity the approach is ideally suited to study macromolecules in different conformational states, such as the Ca^{2+}-release channel in its open (Serysheva *et al.*, 1995) and in its closed state (Orlova *et al.*, 1996). Another advantage of this technique that does not require tilting of the specimen holder is that it is much simpler to evaluate the data to high resolution (10Å and beyond) than when one needs to take defocus gradients in tilted images into account. The future of 3D analysis of single particles clearly lies with zero-tilt techniques, a statement which is underlined by the inventors of the RCT technique who are now also moving rapidly towards our zero-tilt approaches.

Obviously, not all problems with the approach have been solved. For example, it is as yet not quite clear what the optimal size is for the class averages to be used in the angular reconstruction procedures. Too large classes will cover a too large Euler angle range which leads to a low output of information. On the other hand, too small classes become too noisy and are more likely to be assigned an incorrect set of Euler angles. Such unsolved optimization issues will undoubtedly find good theoretical solutions in the future. More pressing than such theoretical issues is the optimization of the electron microscopy and specimen preparation techniques. We currently concentrate our electron microscopical data collection efforts on the "SOPHIE", which is equipped with a super-conducting liquid-helium cooled lens and 200kV field emission gun (FEG) (Zemlin *et al.*, 1996). With this instrument (or rather with its super-conducting lens) it was shown possible to obtain quasi-atomic-resolution 3D reconstructions (Henderson *et al.*, 1990). Of primary importance is also the specimen preparation technique: we have reached high resolution levels of 3D single-particle reconstructions by, for example, embedding the individual molecules in mixtures of glucose and neutral-pH negative stain (Orlova *et al.*, 1997).

In the decade since its unveiling, our angular reconstitution technique has developed explosively and the resolution levels routinely achieved approach the 10Å level. Although such a resolution level is still derided as "blobology" by X-ray crystallographers who prefer to work at the 2-3Å resolution level (see: McRee, 1993), that resolution can be reached without the painful and often prolonged gestation period required to grow crystals. Angular reconstitution thus frees one to focus on the biology of the structure and its relation to function. Finally, no real resolution limits have been identified which would interfere with achieving or even exceeding 5Å resolution (Henderson, 1995). At such resolution levels, angular reconstitution would present a genuine alternative, and not merely a complement or consolation prize, to X-ray crystallography.

Acknowledgments

References

Adrian M, Dubochet J, Lepault J, McDowall AW (1984) Cryo-electron microscopy of viruses. Nature **308**:

32-36.

Bazett-Jones DP, Mendex E, Czarnota GJ, Ottensmeyer FP, Allfrey VG (1996) Visualisation and analysis of unfolded nucleosomes associated with transcribing chromatin. Nucl Acid Res **24**: 321-329.

Bender R, Hellman S, Gordon, R (1970) ART and the ribosome: a preliminary report on the three-dimensional structure of individual ribosomes determined by an algebraic reconstruction technique. J Theor Biol **29**: 483-487.

Beniac DR, Harauz G (1995) Structures of small subunit ribosomal RNAs *in situ* from *Escherichia coli* and *Thermomyces lanuginosus*. Mol Cell Biochem **148**: 165-181.

Blundell TL, Johnson LN (1976) Protein Crystallography. Academic Press, New York. *pages*

Borland L, van Heel M (1990) Classification of image data in conjugate representation spaces. J Optic Soc Am **A 7**: 601-610.

Cejka Z, Santini C, Tognon G, Ghiretti Magaldi A (1991) The molecular architecture of the extracellular hemoglobin of *Ophelia bicornis*: Analysis of two-dimensional crystalline arrays. J Struct Biol **107**: 259-267.

Cejka Z, Kleinz J, Santini C, Hegerl R, Ghiretti Magaldi A (1992) The molecular architecture of the extracellular hemoglobin of *Ophelia bicornis*: Analysis of individual molecules. J Struct Biol **109**: 52-60.

Cheng RH, Reddy VS, Olson NH, Fisher AJ, Baker TS, Johnson JE (1994) Functional implications of quasi-equivalence in a T3 icosahedral animal virus established by cryo-electron microscopy and X-ray crystallography. Structure **2**: 271-282.

Crowther RA (1971) Procedures for three-dimensional reconstruction of spherical viruses by Fourier synthesis from electron micrographs. Phil Trans Roy Soc Lond **B 261**: 221-230.

Crowther RA, DeRosier DJ, Klug A (1970) The reconstruction of a three-dimensional structure from projections and its application to electron microscopy. Proc Roy Soc London **317**: 319-340.

Crowther RA, Kiselev NA, Boettcher B, Berriman JA, Borisova GP, Ose V, Pumpens P (1994) Three-dimensional structure of hepatitis B virus core particles determined by electron cryomicroscopy. Cell **77**: 943-950.

Czarnota GJ, Andrews DW, Farrow NA, Ottensmeyer FP (1994) A structure for the signal sequence binding protein SRP54: 3D reconstruction from STEM images of single molecules. J Struct Biol **113**: 35-46.

Czarnota GJ, Ottensmeyer FP (1996) Structural states of the nucleosome. J Biol Chem **271**: 3677-3683.

DeRosier DJ, Klug A (1968) Reconstruction of three dimensional structures from electron micrographs. Nature **217**: 130-134.

DeRosier DJ, Moore PB (1970) Reconstruction of three-dimensional images from electron micrographs of structures with helical symmetry. J Mol Biol **52**: 355-369.

Dierksen K, Typke D, Hegerl R, Koster AJ, Baumeister W (1992) Towards automatic electron tomography. Ultramicroscopy **40**: 71-87.

Dube P, Tavares P, Lurz R, van Heel M (1993) Bacteriophage SPP1 portal protein: a DNA pump with 13-fold symmetry. EMBO J **15**: 1303-1309.

Dube P, Orlova EV, Zemlin F, van Heel M, Harris JR, Markl J (1995) Three-dimensional structure of keyhole limpet hemocyanin by cryoelectron microscopy and angular reconstitution. J Struct Biol **115**: 226-232.

Dubochet J, Adrian M, Chang J-J, Homo J-C, Lepault J, McDowall A, Schultz P (1988) Cryo-electron microscopy of vitrified specimens. Quart Rev Biophys **21**: 129-228.

Farrow NA, Ottensmeyer FP (1992) A posteriori determination of relative projection directions of arbitrarily oriented macromolecules. J Optic Soc Am **A 9**: 1749-1760.

Farrow NA, Ottensmeyer FP (1993) Automatic 3D alignment of projection images of randomly oriented objects. Ultramicroscopy **52**: 141-156.

Fernández-Moran H, van Bruggen EFJ, Ohtsuki M (1966) Macromolecular organization of hemocyanins and apohemocyanins as revealed by electron microscopy. J Mol Biol **16**: 191-207.

Frank J (1990) Classification of macromolecular assemblies studied as 'single particles'. Quart Rev Biophys **23**: 281-329.

Frank J (1996) Three-dimensional electron microscopy of macromolecular assemblies. Academic Press, New York.

Frank J, Goldfarb W, Eisenberg D, Baker TS (1978) Reconstruction of glutamine synthetase using computer averaging. Ultramicroscopy **3**: 283-290.

Frank J, Verschoor A, Boublik M (1981) Computer averaging of electron micrographs of 40S ribosomal subunits. Science **214**: 1353-1355.

Frank J, Zhu J, Penczek P, Li Y, Srivastava S, Verschoor A, Radermacher M, Grassucci R, Lata RK, Agrawal RK (1995) A model of protein synthesis based on cryo-electron microscopy of the *E. coli* ribosome. Nature **376**: 441-444.

Goncharov AB, Gelfand MS (1988) Determination of mutual orientation of identical particles from their projections by the moments method. Ultramicroscopy **25**: 317-328.

Harauz G (1990) Representation of rotations by unit quaternions. Ultramicroscopy **33**: 209-213.

Harauz G, Ottensmeyer FP (1984a) Direct three dimensional reconstruction for macromolecular complexes from electron micrographs. Ultramicroscopy **12**: 309-319.

Harauz G, Ottensmeyer FP (1984b) Nucleosome reconstruction via phosphorus mapping. Science **226**: 936-940.

Harauz G, van Heel M (1986a) Direct 3D recon-

struction from projections with initially unknown angles. In: Pattern Recognition in Practice II. Gelsema ES, Kanal L (eds). North-Holland Publishing, Amsterdam. pp. 279-288.

Harauz G, van Heel M (1986b) Exact filters for general geometry three dimensional reconstruction. Optik **73**: 146-156.

Harauz G, Borland L, Bahr GF, Zeitler E, van Heel M (1987) Three-dimensional reconstruction of a human metaphase chromosome from electron micrographs. Chromosoma **95**: 366-374.

Henderson R (1995) The potential and limitations of neutrons, electrons and X-rays for atomic resolution microscopy of unstained biological molecules. Quart Rev Biophys **28**: 171-193.

Henderson R, Unwin PNT (1975) Three-dimensional model of purple membrane obtained by electron microscopy. Nature **257**: 28-32.

Henderson R, Baldwin JM, Ceska TA, Zemlin F, Beckman E, Downing KH (1990) Model for the structure of bacteriorhodopsin based on high-resolution electron cryomicroscopy. J Mol Biol **213**: 899-929.

Hoppe W, Gaßmann J, Hunsmann N, Schramm HJ, Sturm M (1974) Three-dimensional reconstruction of individual negatively stained yeast fatty acid synthetase molecules from tilt-series in the electron microscope. Hoppe-Seylers Z Physiol Chem **355**: 1483-1487.

Jap BK, Zulauf M, Scheybani T, Hefti A, Baumeister W, Aebi U, Engel E (1992) 2D crystallization: from art to science. Ultramicroscopy **46**: 45-84.

Kam Z (1980) The reconstruction of structure from electron micrographs of randomly oriented particles. J Theor Biol **82**: 15-39.

Kam Z, Gafni I (1985) Three-dimensional reconstruction of the shape of human wart virus using spatial correlations. Ultramicroscopy **17**: 251-262.

Kleinschmidt AK (1975) Seminar-Bericht: International Seminar on Biomolecular Electron Microscopy. München. Kontron GmbH, Eching-München.

Kühlbrandt W, Downing KH (1989) Two-dimensional structure of plant light-harvesting complex at 3.7Å resolution by electron crystallography. J Mol Biol **207**: 823-828.

Kühlbrandt W, Wang DN, Fujiyoshi Y (1994) Atomic model of plant light-harvesting complex. Nature **367**: 614-621.

Lake JA (1982) Ribosomal subunit orientations determined in the monomeric ribosome by single and by double-labeling immune electron microscopy. J Mol Biol **161**: 89-106.

McRee DE (1993) Practical Protein Crystallography. Academic Press, San Diego.

Misell DL (1978) Image Analysis, Enhancement and Interpretation. North-Holland, Amsterdam.

Moore PB (1995) Ribosomes seen through a glass less darkly. Structure **3**; 851-852.

Öfverstedt LG, Zhang K, Tapio S, Skoglund U, Isaksson LA (1994) Starvation in vivo for aminoacyl-tRNA increases the spatial separation between the two ribosomal subunits. Cell **79**: 629-638.

Oettl H, Hegerl R, Hoppe W (1983) Three-dimensional reconstruction and averaging of 50S ribosomal subunits of *Escherichia coli* from electron micrographs. J Mol Biol **163**: 431-450.

Orlova EV, van Heel M (1994) Angular reconstitution of macromolecules with arbitrary point-group symmetry. In: Proc 13th Intern Congress Electron Microsc. Jouffrey B, Colliex C (eds). Les Editions de Physique, Les Ulis. Vol. 1, pp. 507-508.

Orlova EV, Serysheva II, van Heel M, Hamilton SL, Chiu W (1996) Two structural configurations of the skeletal muscle calcium release channel. Nature Struct Biol **3**: 547-552.

Orlova EV, Dube P, Harris JR, Beckman E, Zemlin F, Markl J, van Heel M (1997) Structure of Keyhole Limpet Hemocyanin type 1 (KLH1) at 15Å resolution by electron cryomicroscopy and angular reconstitution. J Mol Biol **271**: 417-437.

Penczek PA, Grassucci RA, Frank J (1994) The ribosome at improved resolution: new techniques for merging and orientation refinement in 3D cryo-electron microscopy of biological particles. Ultramicroscopy **53**: 251-270.

Penczek PA, Zhu J, Frank J (1996) A common-line based method for determining orientations for N>3 particle projections simultaneously. Ultramicroscopy **63**: 205-218.

Provencher SW, Vogel RH (1988) Three-dimensional reconstruction from electron micrographs of disordered specimens. I. Method. Ultramicroscopy **25**: 209-222.

Radermacher M (1988) Three-dimensional reconstruction of single particles from random and nonrandom tilt series. J Electr Microsc Tech **9**: 359-394.

Radermacher M (1994) Three-dimensional reconstruction from random projections: orientational alignment via Radon transforms. Ultramicroscopy **53**: 121-136.

Radermacher M, Wagenknecht T, Verschoor A, Frank J (1987a) Three-dimensional structure of the large ribosomal subunit from Escherichia coli. EMBO J **6**: 1107-1114.

Radermacher M, Wagenknecht T, Verschoor A, Frank J (1987b) Three-dimensional reconstruction from a single-exposure, random conical tilt series applied to the 50S ribosomal subunit of Escherichia coli. J Microsc **146**: 113-136.

Salzman DB (1990) A method of general moments for orienting 2D projections of unknown 3D objects. Comp Vision, Graphics Image Proc **50**: 129-156.

Saxton WO, Baumeister W (1982) The correlation averaging of a regularly arranged bacterial cell envelope protein. J Microsc **127**: 127-138.

Schatz M, van Heel M (1992) Invariant recognition of molecular projections in vitreous-ice preparations. Ultramicroscopy **45**: 15-22.

Schatz M, Orlova EV, Dube P, Jäger J, van Heel M (1995) Structure of *Lumbricus terrestris* hemoglobin at 30Å resolution determined using angular reconstitution. J Struct Biol **114**: 28-44.

Schatz M, Orlova EV, Dube P, Stark H, Zemlin F, van Heel M (1997) Angular reconstitution in 3D electron microscopy: practical and technical aspects. Scanning Microscopy **Suppl 11**: 179-193.

Serysheva II, Orlova EV, Sherman M, Chiu W, Hamilton S, van Heel M (1995) The skeletal muscle calcium-release channel in its closed state visualized by electron cryomicroscopy and angular reconstitution. Nature Struct Biol **2**: 14-18.

Stark H, Mueller F, Orlova EV, Schatz M, Dube P, Erdemir T, Zemlin F, Brimacombe R, van Heel M (1995) The 70S ribosome at 23Å resolution: fitting the ribosomal RNA. Structure **3**: 815-821.

Stark H, Orlova EV, Rinke-Appel J, Jünke N, Mueller F, Rodnina M, Wintermeyer W, R Brimacombe R, van Heel M (1997) Arrangement of tRNAs in pre- and post-translocational ribosomes revealed by electron cryomicroscopy. Cell **88**: 19-28.

Steinkilberg, Schramm HJ (1980) Eine verbesserte Drehkorrelationsmethode für die Strukturbestimmung (An improved rotational correlation method for structural determinations). Hoppe-Seylers Z Phys. Chemie **361**: 1363-1369.

Unwin PNT, Henderson R (1975) Molecular structure determination by electron microscopy of unstained crystalline specimens. J Mol Biol **94**: 425-440.

Vainshtein BK, Goncharov AB (1986a) Determination of the spatial orientation of arbitrarily arranged identical particles of an unknown structure from their projections. Doklady Akad Nauk USSR **287**: 1131-1134.

Vainshtein BK, Goncharov AB (1986b) Determination of the spatial orientation of arbitrarily arranged identical particles of an unknown structure from their projections. In: Proc XIth Intern Congress on Electron Microsc Kyoto. Imura T, Mause S, Suzuki T (eds). Jap Soc Electron Microsc, Tokyo. pp. 459-460.

Van Dyck D (1989) Three-dimensional reconstruction from two-dimensional projections with unknown orientation, position and projection axis. Ultramicroscopy **30**: 435-438.

Van Heel M (1984a) Multivariate statistical classification of noisy images (randomly oriented biological macromolecules). Ultramicroscopy **13**: 165-184.

Van Heel M (1984b) Three-dimensional reconstructions from projections with unknown angular relationship. In: Proc 8th Eur Congress Electron Microsc. Csanády Á, Röhlich P, Szabó D (eds). Programme Comm 8th Eur Congress Electron Microsc, Budapest, Vol. 2, pp. 1347-1348.

Van Heel M (1987) Angular reconstitution: a posteriori assignment of projection directions for 3D reconstruction. Ultramicroscopy **21**: 111-124.

Van Heel M (1989) Classification of very large electron microscopical data sets. Optik **82**: 114-126.

Van Heel M, Frank J (1980) Classification of particles in noisy electron micrographs using correspondence analysis. In: Pattern Recognition in Practice I. Gelsema ES, Kanal L (eds). North-Holland Publishing, Amsterdam, pp. 235-243.

Van Heel M, Frank J (1981) Use of multivariate statistics in analyzing the images of biological macromolecules. Ultramicroscopy **6:** 187-194.

Van Heel M, Harauz G (1988) Biological macromolecules explored by pattern recognition. Scanning Microsc **Suppl 2**: 295-301.

Van Heel M, Stöffler-Meilicke M (1985) Characteristic views of *E. Coli* and *B. stearothermophilus* 30S ribosomal subunits in the electron microscope. EMBO J **4**: 2389-2395.

Van Heel M, Schatz M, Orlova EV (1992a) Correlation functions revisited, Ultramicroscopy **46**: 307-316.

Van Heel M, Winkler HP, Orlova EV, Schatz M (1992b) Structural analysis of ice-embedded single particles. Scanning Microscopy **Suppl 6**: 23-42.

Van Heel M, Harauz G, Orlova EV, Schmidt R, Schatz M (1996). The next generation of the IMAGIC image processing system. J Struct Biol **116**: 17-24.

Vogel RH, Provencher SW, von Bonsdorff C-H, Adrian M, Dubochet J (1986) Envelope structure of Semliki Forest virus reconstructed from cryo-electron micrographs. Nature **320**: 533-535.

Vogel RH, SW Provencher SW (1988) Three-dimensional reconstruction from electron micrographs of disordered specimens. II. Implementation and results. Ultramicroscopy **25**: 223-240.

Wrigley NG (1975) Reconstruction of single non-periodic macromolecules. In: Image Processing for 2-D and 3-D projections, Digest of Technical Papers, TuD3-1. Stanford University, California.

Yonath A, Berkovitch-Yellin Z (1993) Hollows, voids, gaps and tunnels in the ribosome. Curr Opin Struct Biol **3**: 175-181.

Zemlin F, Beckmann E, van der Mast KD (1996) A 200 kV electron microscope with Schottky field emitter and a helium-cooled superconducting objective lens. Ultramicroscopy **63**: 227-238.

Discussion with Reviewers

R. Hegerl: Notwithstanding the danger of suffering some collateral damage as a spectator in the cross-fire between the parties of angular reconstitution and of random conical tilt (RCT), I think it is not fair to denote the RCT as a tilt series approach associated with radiation damage due to multiple exposure of the specimen.

Authors: Indeed, in our presentation, we did not cover that issue in sufficient detail. The point we are trying to make is that the second exposure, from which the alignment and angular parameters are deduced, has suffered an additional exposure and thus the parameters are not as good as parameters taken from the exposure. Moreover, the macroscopic tilt between the exposures introduces a new series of problems we discussed in the text. It cannot have escaped the attention of the neutral spectators in the battle between the approaches, that the remedy for the problems ("AZT", see above) with the RCT approach proposed by the Albany group is, in fact, a minor variant of the angular reconstitution technique.

O. Saxton: In spite of the assertion that "no theoretical limits are yet in sight", there must be a dependence on scattering power, specimen size and/or radiation dose. Can any of this be expressed simply?

Authors: Indeed there must be. In Henderson (1995), the issue is discussed in some detail and the conclusion is that one needs at least 10000 molecular images of a reasonably sized protein to be able to find its atomic-resolution structure. For the time being, that study suffices although it will be necessary to revisit the issue once the question gets to be more opportune, that is, once the resolution level of the approach routinely reaches levels below, say, 10Å. The assumptions made in Henderson (1995) do not fully cover our procedural practices and we will thus have to look at the issue again in the future.

O. Saxton: How is the entire bootstrapping started? As described, the procedure assumes an existing reconstruction for alignment purposes.

Authors: It is in the refinement part of the procedures that most of the fine detail emerges from the data so there is some justification to present the procedures as we did here. In the accompanying paper we follow the actual procedures in the correct order and the 3D reconstruction appears only at the later phases of the story.

O. Saxton: Can you say something specific about the relative merits of the common-lines detection in real space and Fourier space?

Authors: There are advantages to the real-space angular reconstitution technique although it is, in principle, the real-space equivalent of the Fourier space common central lines technique. The advantages lie in being able to directly visualize the real data as opposed to complex data. However, the angular reconstitution approach (van Heel, 1987), is more than the pure Euler angle assignment as is discussed in the paper. The overall approach includes normally also the grouping into classes of the raw molecular images and it thus allows one to considerably reduce the noise levels prior to the Euler angle assignment. Although this has not yet been used very extensively for the analysis of icosahedral viruses, this possibility bears a potential to reach higher resolution levels than have been achieved using typically 20-100 viral images with the common-lines programs. Moreover, the angular reconstitution programs are formulated for general pointgroup symmetries which gives a flexibility that is not present in the conventional common-lines programs. One may, for example, first analyze a phage head with icosahedral symmetry, and later relax that symmetry to C5 in order to accommodate the portal protein of which there is only one copy, in the five-fold symmetric environment of the portal vertex.

O. Saxton: Surely angular reconstitution (AR) fails completely if a molecule has one preferred orientation on the support film? And common-line detection (relying on so few of the data) surely fails a much higher minimum dose than that at which the RCT approach fails? And the likelihood of mis-assignment of angles is surely greater in AR than in RCT, where at least one is directly observed?

Authors: Many questions at once! (a) The AR approach will indeed fail if there is only one preferred orientation of the molecule. However, we find that it is not all that difficult to ensure a more random distribution of the particles. Moreover in cases where there is only one specific view, the interactions between the particles and the substrate are so strong and deforming that one can hardly be interested in interpreting the resulting 3D reconstruction in terms of the biology of the molecule. (b) The AR approach still functions at very low SNR levels because of the use of class averages. We would even go so far as to state that the AR approach still works at noise levels where the RCT approach has already collapsed. (c) The first alignments with the AR approach very often are "alignments by classification" (Dube *et al.*, 1993) which alignments obey statistics which are different from the CCF statistics between two raw, noisy molecular images. Again, we expect significant misalignments only to occur at SNR levels where the RCT approach has already collapsed. Indeed, as is discussed in our paper, our honored competitors have now implemented a number of angular reconstitution variants (see "AZT" in the main text) as stand-alone techniques or

as techniques to improve on the RCT results.

O. Saxton: Can you explain simply why Angular Reconstitution may have a higher resolution than other approaches?

Authors: This may sound redundant, but the only other current technique that is likely to reach a very much higher resolution level of, say, better than ~10Å, is the Fourier space common central lines approach exploiting the 60-fold redundancy of icosahedral viruses. We think that for all point-group symmetries it is better to work with very large data sets and class averages to reach extremely high resolutions. For icosahedral particles, however, one may be able to exploit the built-in 60-fold redundancies to reach quasi-atomic resolution without resorting to class averages. Indeed, we believe in our technique!